# A quasi-crystal model of collagen microstructure based on SHG microscopy

**Pu Xu[1,3*], Eleanor Kable[1], Colin J. R. Sheppard[2], and Guy Cox[1]**

[1]*Australian Key Centre for Microscopy and Microanalysis, University of Sydney, NSW 2006, Australia*

[2]*Division of Bioengineering, National University of Singapore, Singapore 117576*

[3]*Key Laboratory of Ecophysics, Department of Physics, Shihezi University, Shihezi 832000, China*

[*]*E-mail: xupu@tsinghua.org.cn*

Received April 13, 2009

Second harmonic generation (SHG) results from molecules which are polarized by an external electric field often provided by an intense laser beam. The polarizability depends on firstly the intrinsic structural properties of the substance and hence the second-order nonlinear susceptibility, and secondly the intensity and polarization direction of the incident light. The polarization characteristics of the beam are therefore of interest. In this letter, we discuss some considerations in SHG microscopy of collagen when the incoming beam is circularly polarized, and present some supporting results as well as a numerical analysis. We propose a quasi-crystal model of collagen microstructure in an effort to further our understanding on this protein.

*OCIS codes:* 180.0180, 190.0190, 260.0260.

*doi: 10.3788/COL20100802.0213.*

When molecules are polarized by an electric field exerted on them, their subsequent dipole radiation contains harmonic components, namely second, third and higher harmonic generation[1]. The second harmonic generation (SHG) is generally the strongest of these when the material lacks structural centro-symmetry, typical examples of these include solid noncentrosymmetric crystals[2].

SHG has been employed in microscopy based on intense laser illumination[3,4], and has produced many promising results[5−7], including biological/biomedical applications[8−11]. While in perfect periodical structures such as single crystals, the polarizability of the substance is uniform throughout; in partially regular structures or structures containing regular components whereas these components are randomly scattered in space, it is natural to ask how the change in polarizability in spatial terms influences the signal output which is used to form images.

Atoms, when forming molecules in ionic bond or valence bond, often exhibit electric polarities. When this polarity is in line with the electric field of incoming light, it is polarized most strongly; the degree of polarizability will decrease with the increase of the angle between the external field and the internal polarity, and reaches zero when they become perpendicular. When semi-regular structures are under a microscope, we would like molecules of all orientations to be excited. A circularly polarized beam offers electric field around 360° and hence offers an attractive candidate for studying these semi-regular structures such as many biological specimens.

The microscope used was an inverted microscope (DMIRBE, Leica, Germany), fitted with a spectrometric confocal head (Leica Microsystems, Germany). The laser is a coherent Mira Ti: sapphire system, tunable between 700 and 1000 nm, operating in the femtosecond regime and pumped by a 5-W solid-state laser (Verdi, Coherent Scientific, USA). All additional detectors and optical equipment were supplied by Leica Microsystems, with the exception of the additional filters and dichroics, supplied by Chroma Inc.

To establish the significance of being able to manipulate the polarization plane of light entering the medium, we conducted two sets of experiments on single crystal and biological samples.

We fixed the relative orientation between the sample and the linear polarization plane of the laser beam, and rotated the analyser in front of the receiving optics (but after the sample). After each such cycle we changed the relative angle between the sample and the beam, i.e., either the sample or the polarization plane of the beam was rotated and carried out the analyser cycle again. This sequence was repeated until all combinations of the two angles were investigated.

The first set of images is high $\chi^{(2)}$ single crystal of potassium dihydrogen phosphate (KDP) at 100-$\mu$m thickness, as shown in Fig. 1. It can be seen that not only the sample is best excited when the relative angle between itself and the incident beam remained at one constant value, but also the second harmonic (SH) emission is linearly polarized and the polarization plane is determined by the orientation of the sample, regardless of the incident light.

Figure 2 shows the similar phenomenon when a piece of biological specimen, a sliced bone sample, is imaged. Collagen in the bone is a strong generator of the SH[8,12−14]. We extracted four images to show the linkage between the input and the sample, and the sample and the output. The upper two images were acquired with a constant angle between the sample and the incident polarization with two analyser positions allowing emission to pass at angle of 90° to one another; the bottom two were acquired with a constant angle between sample and analyser but using two directions of

 

the polarization plane of the incident beam, at 90° to one another. Both pairs of images show clear contrast at orthogonal polarizations, nontheless, due to the wavy nature of the specimen, and the angular error at rotation of the specimen in the lower panel of images, many SH visible structures are not strictly horizontal/vertical, but tilted.

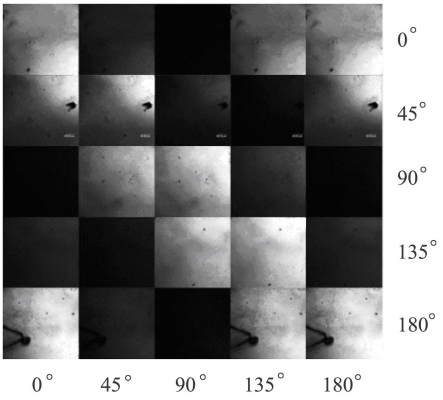


Fig. 1. Matrix of KDP single crystal SHG intensity variation. From left to right, analyser at angles of 0°, 45°, 90°, 135°, and 180°; From top to bottom, sample is rotated by 0°, 45°, 90°, 135°, and 180°. The mark on the last row of images is a contaminant.

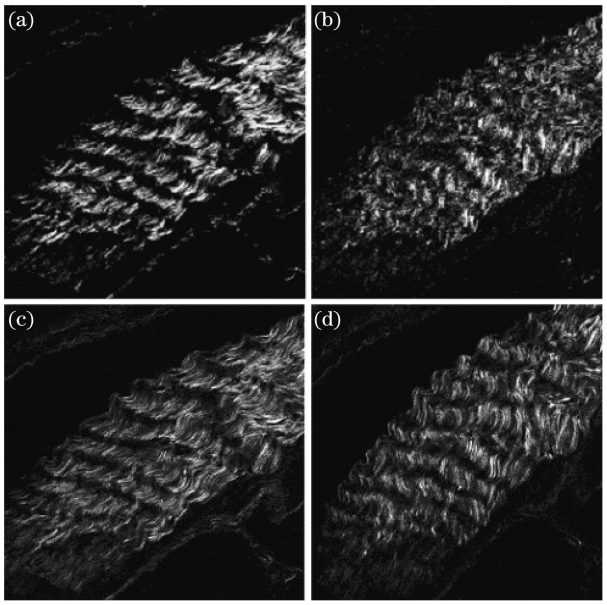


Fig. 2. SHG images acquired at combination of sample-input angles and sample-output angles. Top row: sample-input fixed, analyser rotated by 90° between (a) the left and (b) the right images; bottom row: sample-output fixed, polarization of input rotated by 90° between the left (c) and the right (d) images. Image width in each case is 187.5 $\mu$m.

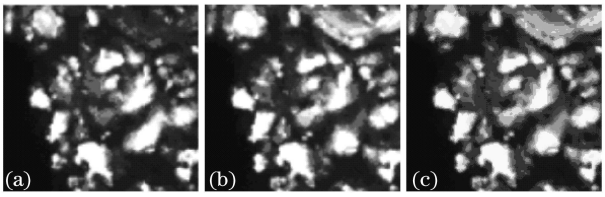


Fig. 3. KDP crystal particles imaged under SHG microscope. (a) Linearly and (b) circularly polarized input; (c) the two images merged with CP in green and LP in red. Image width in each case is 37.5 $\mu$m.

Figures 3 and 4 present a comparison between images acquired using linearly polarized input against circularly polarized. In Fig. 3, ground KDP particles were imaged clearly, many particles were imaged more brightly with the circularly polarized input, particularly in the top area of the images.

Figure 4 compares microscopic images of a biological specimen (collagen) where circularly polarized light revealed the overall structure of the investigated area much better than the linearly polarized light, since collagen fibers at different orientations show similar intensities.

When we analyze the polarization property of the SH under circularly polarized incident beam, we find interestingly that not only features in the specimen are better excited, but also the emission seems to behave in the similar way, as shown in Fig. 5.

From the left column of images, we can see that the SH is predominantly linearly polarized at an angle of 0° which is parallel to the polarization of the incident beam; from the right column of images, we can see that the SH has components at every polarization angle with approximately equal intensity, hence whatever filter angle is set by the analyser, we see images with same clarity. In other words, the orientation of the collagen no longer seems to determine the polarization of the harmonic.

In optical SHG microscopy, the specimen is generally thin, ranging from 100 nm to 10 mm. Under this condition, we can simplify the situation by neglecting the birefringence of the specimen. In semi-regular structures, we assume that the crystallites are big enough to generate observable SH, while the sample is small enough to be, overall, amorphous. Molecules in the crystallites would only be polarized, but would have no freedom to realign.

Suppose we have a linearly polarized beam and a perfectly linearly oriented structure (Fig. 6(a)). If the orientation of the structure is parallel with the polarization

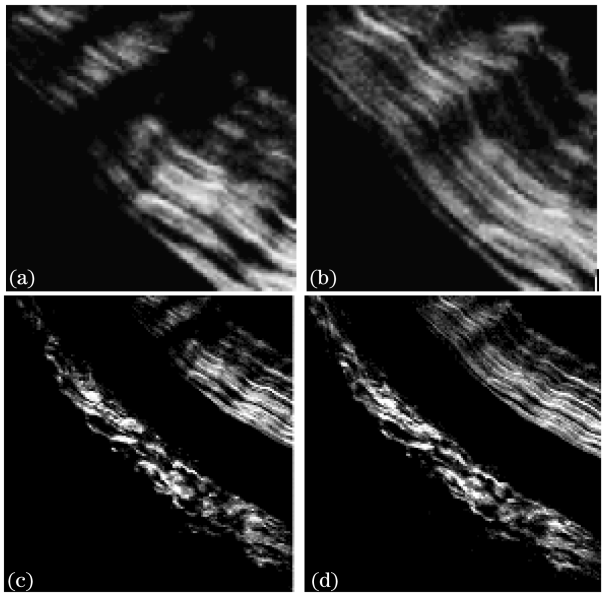


Fig. 4. Sliced bone sample imaged under SHG microscope.

Comparison between (a, c) linearly and (b, d) circularly polarized input. Image width in each case is 187.5 $\mu$m.

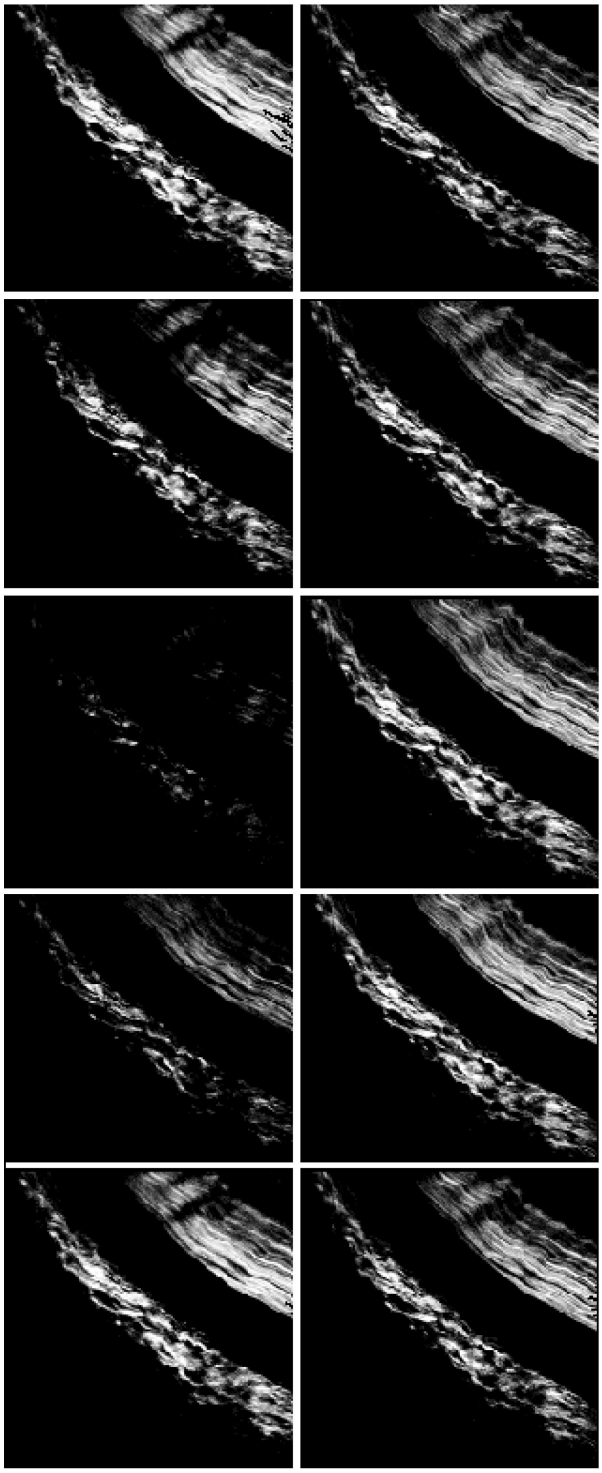

Fig. 5. Images taken with linearly polarized light (left column) compared with those obtained using circularly polarized light (right column). The analyser was at angles of 0°, 45°, 90°, 135°, and 180° for each row from top to bottom. In the linear input case, the plane of polarization was parallel with the 0° analyser angle of 0°.

plane of the light field, each dipole in the medium would be maximally polarized; if, on the other hand, the alignment of the dipoles is at an angle with the field, the level of polarization would be decreased. If the dipoles are omnidirectional in the medium, those in line with the light field will be maximally polarized, others polarized to smaller amplitudes depending on their orientation, and those aligned perpendicular to the field would appear invisible to the light and would emit no SH at all.

Suppose now that we have a circularly polarized beam and an arbitrary structure (Fig. 6(b)). If the structure is a linear one, no matter what its position is relative to the beam, it will get excited by the circularly polarized beam just as in the case of linearly polarized input. If the structure is omnidirectional, however, each dipole would be polarized at certain instance while the circularly polarized wave packet passes through, i.e., the level of polarization of each dipole is independent of the relative angle between the axis of the dipole and the electric field vector. In other words, the only factor that determines the polarization of each dipole is the dipole's intrinsic property.

So far, from a single dipole point of view, circularly polarized light has every advantage over its linearly polarized counterpart. But we need to take another major factor into account, the coherent scattering of the harmonics. Single molecule SHG is often too weak to be observed, therefore coherent scattering is important in building up the overall power of the SH at output. An immediate point is that a completely turbid medium will not offer any opportunity for SHG to be coherently scattered, and circularly polarized input will not do better than linear polarization. In the case of semi-regular structures, it is highly possible that those molecules aligned in the same orientation could generate SH coherently, and consequently give stronger signals.

A circularly polarized electric field can be written in the sum of two linear components as

$$E = \mathbf{x}Ex(z,t) + \mathbf{y}Ey(z,t), \tag{1}$$

where $\mathbf{x}$ and $\mathbf{y}$ denote unit vectors along two axis in the transverse plane of laser beam.

In general case, second-order polarization $P$ is expressed by

$$P = \chi^{(2)}EE/2, \tag{2}$$

where $\chi^{(2)}$ is the second-order optical nonlinear susceptibility of the medium and $E$ is the applied electrical field. To rewrite it in Cartesian components form as

$$\begin{pmatrix} P_x \\ P_y \\ P_z \end{pmatrix} = \begin{pmatrix} d_{11} & d_{12} & d_{13} & d_{14} & d_{15} & d_{16} \\ d_{21} & d_{22} & d_{23} & d_{24} & d_{25} & d_{26} \\ d_{31} & d_{32} & d_{33} & d_{34} & d_{35} & d_{36} \end{pmatrix} \times \begin{pmatrix} E_x^2 \\ E_y^2 \\ E_z^2 \\ 2E_zE_y \\ 2E_zE_x \\ 2E_xE_y \end{pmatrix}. \tag{3}$$

We have described in previous work[15] that different types of collagen fibers exhibited different SHG polarization, we hence proposed a quasi-hexagonal crystal model for collagen with symmetry group $\bar{6}$m2. We chose the crystallographic approach against a molecular

approach[16], because we believe that the observable fibrils were already a pack of tens or hundreds of tropocollagen molecules. The second-order nonlinear susceptibility

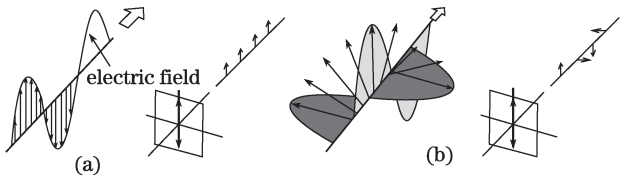


Fig. 6. (a) Linearly polarized light (left) incident on a linear structure (right) with dipole orientation parallel with the polarization plane of the light; (b) circularly polarized light (left) incident onto a non-periodical structure (right) with dipole at omnidirectional angles with the polarization plane of the light.

of group $\overline{6}$m2 can be reduced to

$$\begin{pmatrix} 0 & 0 & 0 & 0 & 0 & d_{16} \\ d_{16} & -d_{16} & 0 & 0 & 0 & 0 \\ 0 & 0 & 0 & 0 & 0 & 0 \end{pmatrix} \quad (4)$$

or

$$\begin{pmatrix} d_{11} & -d_{11} & 0 & 0 & 0 & 0 \\ 0 & 0 & 0 & 0 & 0 & -d_{11} \\ 0 & 0 & 0 & 0 & 0 & 0 \end{pmatrix}. \quad (5)$$

By doing the coordinate translation, it works out that in either orientation, corresponding to (4) and (5), there is SH polarization along the optical axis direction, which is given by $d_{16}E_y^2$ or $-d_{11}E_x^2$.

Since a transverse polariser/analyser would not differentiate a $z$-axis dipole radiation, we observed the same image regardless of the polarization angle; moreover, in circular polarization case, both $E_x$ and $E_y$ are non-zero, therefore no matter which orientation the fibrils happen to sit, the axial SH remains.

Lastly, our excitation beam is a train of short pulses, at ∼100 fs duration with 80 MHz repetition rate; our acquisition, on the other hand, is at ∼4 frames per second, so every image is a statistical average of hundreds of pulsed SH emissions depending on the acquisition time.

In conclusion, circularly polarized light has shown advantages in imaging applications of SHG over linearly polarized light. Semi-regular structures are better excited under circularly polarized light and result in better images. A numerical analysis implies that a quasi-crystal microstructure may lead to a better understanding of soft condensed matter, collagen in this case.

This work was supported in part by Australian Research Council Research, Infrastructure, Equipment, and Facilities (No. R00002784) and Australian Research Council Discovery (No. DP0210312).

## References

1. P. A. Franken, A. E. Hill, C. W. Peters, and G. Weinreich, Phys. Rev. Lett. **7,** 118 (1961).
2. T. Petrallimallow, T. M. Wong, and J. D. Byers, J. Phys. Chem. **97,** 1383 (1993).
3. R. Hellwarth and P. Christensen, Opt. Commun. **12,** 318 (1974).
4. P. Stoller, B. Kim, A. Rubenchik, K. Reiser, and L. B. DaSilva, J. Biomed. Opt. **7,** 205 (2002).
5. J. N. Gannaway and C. J. R. Sheppard, Opt. Quantum Electron. **10,** 435 (1978).
6. R. Gauderon, P. B. Lukins, and C. J. R. Sheppard, Micron. **32,** 685 (2001).
7. L. Moreaux, O. Sandre, S. Charpak, M. Blanchard-Desce, and J. Mertz, Biophys. J. **80,** 1568 (2001).
8. G. Cox, E. Kable, A. Jones, I. Fraser, F. Manconi, and M. Gorrell, J. Structural Biol. **141,** 53 (2003).
9. P. Campagnola, H. A. Clark, W. A. Mohler, A. Lewis, and L. M. Loew, J. Biomed Opt. **6,** 277 (2001).
10. P. J. Campagnola, A. C. Millard, M. Terasaki, P. E. Hoppe, C. J. Malone, and W. A. Mohler, Biophys. J. **82,** 493 (2002).
11. W. R. Zipfel, R. M. Williams, R. Christie, A. Y. Nitikin, B. T. Hyman, and W. W. Webb, Proc. Natl. Acad. Sci. **100,** 7075 (2003).
12. I. Freund, M. Deutsch, and A. Sprecher, Biophys. J. **50,** 693 (1986).
13. E. Georgiou, T. Theodossiou, V. Hovhannisya, K. Politopoulos, G. S. Rapti, and D. Yova, Opt. Commun. **176,** 253 (2000).
14. S. Roth and I. Freund, Biopolymers **20,** 1271 (1981).
15. P. Xu, G. Cox, J. Ramshaw, P. Lukins, and C. Sheppard, Proc. SPIE **5323,** 343 (2004).
16. S. W. Chu, S. Y. Chen, G. W. Chern, T. H. Tsai, Y. C. Chen, B. L. Lin, and C. K. Sun, Biophys. J. **86,** 3914 (2004).